

# Analog Raychaudhuri equation in mechanics

Rajendra Prasad Bhatt\*, Anushree Roy and Sayan Kar†

*Department of Physics, Indian Institute of Technology Kharagpur, 721 302, India*

## Abstract

Usually, in mechanics, we obtain the trajectory of a particle in a given force field by solving Newton's second law with chosen initial conditions. In contrast, through our work here, we first demonstrate how one may analyse the behaviour of a suitably defined family of trajectories of a given mechanical system. Such an approach leads us to develop a mechanics analog following the well-known Raychaudhuri equation largely studied in Riemannian geometry and general relativity. The idea of geodesic focusing, which is more familiar to a relativist, appears to be analogous to the meeting of trajectories of a mechanical system within a finite time. Applying our general results to the case of simple pendula, we obtain relevant quantitative consequences. Thereafter, we set up and perform a straightforward experiment based on a system with two pendula. The experimental results on this system are found to tally well with our proposed theoretical model. In summary, the simple theory, as well as the related experiment, provides us with a way to understand the essence of a fairly involved concept in advanced physics from an elementary standpoint.

---

\* Present Address: Inter-University Centre for Astronomy and Astrophysics, Post Bag 4, Ganeshkhind, Pune 411 007, India

†Electronic address: bhatttrajendra1997@gmail.com, anushree@phy.iitkgp.ac.in, sayan@phy.iitkgp.ac.in

## I. INTRODUCTION

Imagine two pendula of the same length hung from a common support. Let us give different initial displacements to the bobs and set them in motion (in a single vertical plane) with different initial velocities (see Figure 1). It is obvious that they will strike each other after a finite time. What does this time of striking/meeting depend upon? How does one develop a general theoretical model for such scenarios (with several simple pendula or for other systems) and also set up a simple experiment? Our aim, in this article, revolves around such issues and questions which, to the best of our knowledge, have not been addressed in standard texts on mechanics [1, 2]. In particular, we concentrate on the collective behaviour of families of trajectories of a given mechanical system.

It turns out that such studies are directly related to the well-known Raychaudhuri equation [3] (also see [4]) which arises in Riemannian geometry and is used in General Relativity [5–8]. There too, the central aim is to analyse the behaviour of a bunch of trajectories (geodesics). In General Relativity, or any metric theory of gravity, a curved spacetime represents a gravitational field. Freely falling (no other non-gravitational forces) trajectories of test particles (massive or massless) are the *extremal* curves or *geodesics* in a curved spacetime. A family of such non-intersecting geodesics defines a *geodesic congruence*. It is therefore natural to ask—what happens to an *initially converging* geodesic congruence? The answer leads us to the *focusing theorem* which states the following: *under specific conditions (known in technical jargon as the convergence condition and the absence of vorticity/rotation), the family of geodesics must end up meeting (focusing) within a finite value of a parameter  $\lambda$  (similar to ‘time’ in mechanics,  $\lambda$  labels points on the geodesics).* Thus, focusing leads to a *breakdown* of the definition of a congruence.

The term *focusing* is quite commonly known and used in geometrical optics. Its usage here, is in the sense that trajectories of mechanical systems may meet within a finite value of time. The meeting point is the *focus* or a *focal point/curve*. In optics, trajectories are light rays and focusing may be related to the occurrence of caustic curves where light intensities are enhanced drastically. [12, 13].

What does the focusing theorem signify in the context of General Relativity? Since the Einstein field equations relate geometry to matter, the *geometric* condition for focusing may be translated to that for matter [5, 6]. Such a condition, simply stated, is just the physical

requirement of positive energy density. Therefore, the attractive nature of gravity leads to focusing— an almost obvious conclusion! Further, it is possible that the focal point of a family/congruence is a spacetime singularity (eg. the big-bang or a black hole singularity, where one encounters extreme spacetime curvature or infinite matter density). Hence the role of the *Raychaudhuri equation and the focusing theorem* as crucial ingredients in the proofs of the celebrated singularity theorems of Penrose [9] and Hawking [10], [11].

However, it is important to realise that focusing as such, can be completely benign. The focal point need not be a spacetime singularity, but only a point/curve where the converging family of trajectories meet. This brings us back to the question asked in the first paragraph above—when does meeting happen, what are the conditions? It is this point of view (i.e. benign focusing) which we take forward while developing our analog Raychaudhuri equation in mechanics [14].

In elementary mechanics, given a force field or a potential we can, from Newton’s second law, obtain a precise trajectory, once appropriate initial conditions are provided [1, 2]. To develop the approach highlighted above, we need to properly define a family of trajectories as well as variables associated with the collection, as a whole. Once such variables are

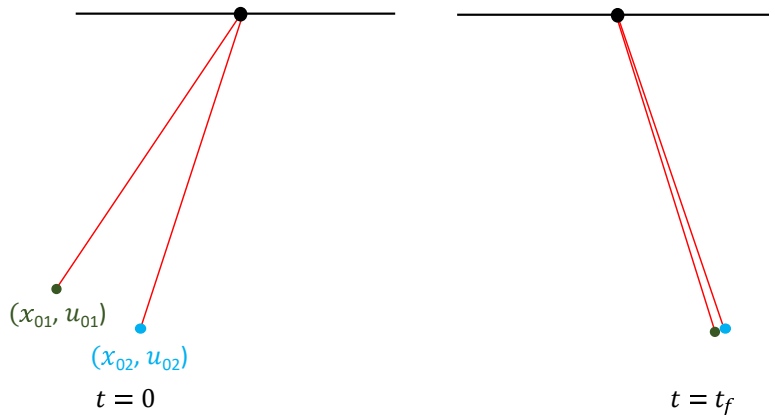


FIG. 1: Simple pendula: Here  $x_{01}, x_{02}$  are initial positions and  $u_{01}, u_{02}$  are initial velocities of the two bobs (figure on the left). Meeting of the bobs at  $t = t_f$  (figure on the right).

defined, their values at each instance of time will show the nature of evolution of the family, as a single entity. The question of convergence/divergence or the meeting/avoidance of trajectories in finite time can therefore be addressed and linked to the behaviour of such variables [14]. Varying the initial positions and momenta (velocities) around specific values yields different trajectories in configuration space. One useful variable for a family is the

gradient of the velocity, known as the ‘expansion’, which, as we will see, appears in the Raychaudhuri equation and is central to our forthcoming discussion.

Our article is arranged as follows. In the next section (Section II), we briefly outline, recalling earlier work [14], the theoretical model related to the behaviour of a family of trajectories in mechanics. The definitions of the meeting time as well as the expansion are both introduced here. Thereafter, in Section III, we move on to the experiment, elaborating on various details of experimentation. We report on how the theoretical model tallies with our experimental findings in Section IV. A briefing on the correspondence between mechanical systems and relativity *vis-a-vis* the Raychaudhuri equation and focusing, appears in Section V. Finally, we conclude with remarks on possible future investigations.

## II. THEORETICAL MODEL

The equation of motion of a particle of unit mass, in the force field  $f$  (with a potential  $V$ ), in one dimension, is given as [1, 2]:

$$\dot{u} = \ddot{x} = -\frac{\partial V}{\partial x}. \quad (1)$$

Given the potential or the force field, as well as initial ( $t = 0$ , say) conditions on position and velocity ( $x = x_0$ ,  $u = u_0$  at  $t = 0$ ), one can write down the expression for  $x(t)$  (assuming integrability). A different set of initial conditions ( $x = x_0 + \Delta x_0$ ,  $u = u_0 + \Delta u_0$  at  $t = 0$ ) will result in a *different trajectory*. Thus, fixing the ratio of the difference in initial velocity and the difference in initial position of the trajectories ( $\frac{\Delta u}{\Delta x}$  at  $t = 0$  or  $\frac{\Delta u_0}{\Delta x_0}$ ), we can generate a family of trajectories for the mechanical system (see Figure 2). Each trajectory in the family has a different initial position and initial velocity, but, for the collection, the ratio  $\frac{\Delta u}{\Delta x}$  at  $t = 0$  is fixed.

One may further ask about the behaviour of  $\frac{\Delta u}{\Delta x}$  for this family, at different future time instances. This leads us towards the analysis of the kinematics of the family of trajectories, as a whole. We define a new variable  $\theta(t)$  (essentially, the ratio  $\frac{\Delta u}{\Delta x}$  at each time, with a fixed initial value and w.r.t. a single reference trajectory) for the family.  $\theta(t)$  is named the expansion [14] and is defined as:

$$\theta(t) = \frac{\partial u}{\partial x}. \quad (2)$$

It is obvious that  $\theta(t)$  at each  $t$ , is the gradient of the velocity of neighboring trajectories in

the family w.r.t. a single reference trajectory[14]. More rigorously one should write  $\theta(x(t))$ , i.e. its time-dependence is through  $x(t)$ . We will however continue using  $\theta(t)$  below with the understanding that it is actually  $\theta(x(t))$ .

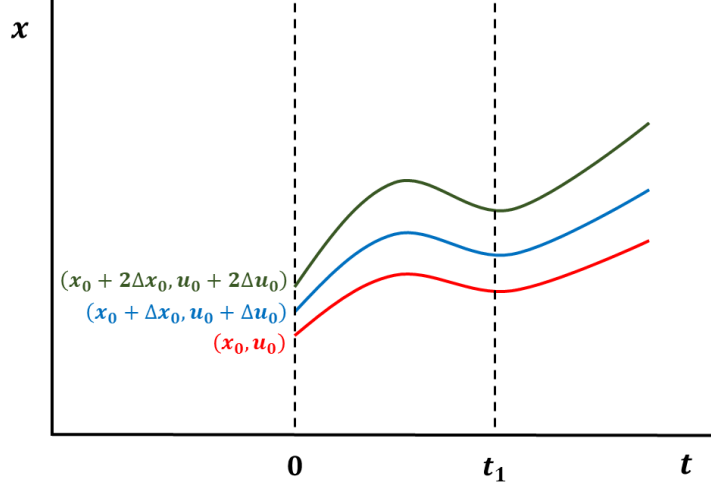


FIG. 2: Qualitative plot of a family of trajectories (constructed w.r.t. the reference curve (red)) for an arbitrary system. Here, the initial position and initial velocity of the trajectories have been written in brackets with the same color at the left side of the  $t = 0$  dashed line as (initial position, initial velocity). The initial expansion (expansion  $\theta(t)$ ) at  $t = 0$  is  $\frac{\Delta u_0}{\Delta x_0}$ . At a later time (say  $t_1$ ), the expansion  $\theta(t)$  is calculated by the ratio of difference in velocity and difference in position of the trajectories ( $\frac{\Delta u}{\Delta x}$ ) at that time.

Next, we ask, what is the differential equation obeyed by  $\theta(t)$ ? Since  $\frac{d}{dt} \equiv \frac{dx}{dt} \frac{\partial}{\partial x}$  (see discussion later on using the convective derivative) we have,

$$\frac{d\theta}{dt} = u \frac{\partial \theta}{\partial x} = \frac{\partial}{\partial x} (u\theta) - \theta^2, \quad (3)$$

and

$$u\theta = u \frac{\partial u}{\partial x} = \frac{du}{dt} = f_{ext} = -\frac{\partial V}{\partial x}, \quad (4)$$

where we have used the equation of motion (1). Thus, the final differential equation obeyed by  $\theta(t)$  is,

$$\frac{d\theta}{dt} + \theta^2 = -\frac{\partial^2 V}{\partial x^2}. \quad (5)$$

In some problems, we may not know a Lagrangian or the potential function though the equation of motion may exist. This includes non-potential/non-conservative force fields [14].

In such cases, the equation for  $\theta(t)$  is,

$$\frac{d\theta}{dt} + \theta^2 = \frac{\partial f_{ext}}{\partial x}. \quad (6)$$

One may question the usage of the directional derivative  $\frac{d}{dt} = u \frac{\partial}{\partial x}$ , as opposed to the convective derivative, i.e.  $\frac{d}{dt} = \frac{\partial}{\partial t} + u \frac{\partial}{\partial x}$ . It is easy to check that such a change does not affect the final equation for  $\theta$ . In particular, assuming the Euler equation in one space dimension,

$$\frac{\partial u}{\partial t} + u \frac{\partial u}{\partial x} = f \quad (7)$$

instead of Newton's second law, one can obtain the same evolution equation for  $\theta$  (i.e.  $\frac{\partial u}{\partial x}$ ). In the case of the pendula or simple harmonic oscillators (with  $f = -\alpha^2 x$ ), the Euler equation has a simple solution:

$$u(x, t) = \alpha x \cot(\alpha t + \beta) \quad (8)$$

which represents the velocity field ( $\beta$  is a constant). The integral curves of this velocity field (obtained from  $\frac{dx}{dt} = u$ ) are,

$$x(t) = C \sin(\alpha t + \beta) \quad (9)$$

where  $C$  is a constant. One can relate the constants  $\beta$  and  $C$  to initial conditions on  $x$  and  $u$ , when choosing a *specific, single curve* in the family. With a fixed initial  $\theta$ , one can obtain its evolution as well as the evolution equation, directly from the velocity field too. Alternatively, as in the preceding discussion here, one may obtain the time evolution of  $\theta$  (i.e.  $\frac{\partial u}{\partial x}$ ) by transporting  $\frac{\partial u}{\partial x}$  in time starting from a fixed initial value. Both approaches eventually yield the same final result, i.e. the same equation for  $\theta$ . Thus, it is clear that the time-dependence of  $\theta$  is *through* the time-dependence of  $x(t)$ , and is not explicit.

### A. Notion of meeting of trajectories

Let us now develop the notion of meeting of trajectories. As stated just above, the trajectory  $x(t)$  has an initial position  $x_0$  and initial velocity  $u_0$ . Further, name the trajectory with initial position  $x_0 + \Delta x_0$  and initial velocity  $u_0 + \Delta u_0$  as  $x'(t)$ . One can write,

$$\Delta u_0 = \left. \frac{\partial u}{\partial x} \right|_{(x=x_0, t=0)} \cdot \Delta x_0 = \theta_0 \Delta x_0,$$

where  $\theta_0$  is termed as the initial expansion [14] and is given as:

$$\theta_0 = \left. \frac{\Delta u}{\Delta x} \right|_{(t=0)}. \quad (10)$$

If at time  $t = t_f$ , the two trajectories meet, then,

$$x(t_f) = x'(t_f).$$

From this condition, we can find the initial value of  $\theta_0$  for which two trajectories may meet at some future time  $t_f$ . Notice that  $\theta_0$  depends on the ratio of  $\Delta u$  and  $\Delta x$  at  $t = 0$ . Thus, there are infinite possible values of  $\Delta u$  and  $\Delta x$  at  $t = 0$ , which have the same  $\theta_0$ , thereby defining a family. It may also happen that the family of trajectories never meet. In such a case, there is no finite value for the meeting time [14].

In one dimension, we can also write  $\theta(t)$  as,

$$\theta(t) = \frac{\partial u}{\partial x} \approx \frac{1}{\Delta x} \frac{d\Delta x}{dt}. \quad (11)$$

Thus, it may be interpreted as the fractional rate of change of separation between two trajectories [14]. Further rewriting and integrating gives,

$$\int \frac{d\Delta x}{\Delta x} = \int \theta(t) dt,$$

which implies,

$$\Delta x = \Delta x_0 . e^{\int_0^t \theta(t) dt}. \quad (12)$$

Hence, the divergence or convergence of the family of trajectories is related to the values of  $\theta(t)$ . If  $\theta(t) \rightarrow -\infty$  in finite time, then  $\Delta x \rightarrow 0$  in finite time, i.e., trajectories converge. This is the well-known notion of meeting/focusing of a family of trajectories (see the penultimate section where the analogy with geodesic congruences is discussed). If  $\theta(t) \rightarrow \infty$  in finite time, then  $\Delta x \rightarrow \infty$  in finite time, i.e. the family of trajectories diverge. Such a behaviour is termed defocusing.

We now move on to discuss the simple harmonic oscillator (or, equivalently, simple pendula) [14]. The equation of motion here is:

$$\ddot{x} = -\alpha^2 x, \quad (13)$$

where  $\alpha$  is the angular frequency. The general solution turns out to be:

$$x(t) = x_0 \cos(\alpha t) + \left( \frac{u_0}{\alpha} \right) \sin(\alpha t), \quad (14)$$

and the velocity  $\dot{x} = u$  is given as,

$$u(t) = -\alpha x_0 \sin(\alpha t) + u_0 \cos(\alpha t). \quad (15)$$

The initial conditions are  $x(t)|_{(t=0)} = x_0$ ,  $u(t)|_{(t=0)} = u_0$ .

Let us assume we have two pendula with initial positions  $x_0$  and  $x_0 + \Delta x_0$  and initial velocities  $u_0$  and  $u_0 + \Delta u_0$ , respectively. Here  $x(t)$  may be taken as the variable ‘length  $\times$  angle’. Using  $x(t)$  (Equation 14), we obtain,

$$\begin{aligned} x_1(t) &= x_0 \cos(\alpha t) + \left(\frac{u_0}{\alpha}\right) \sin(\alpha t), \\ x_2(t) &= (x_0 + \Delta x_0) \cos(\alpha t) + \left(\frac{u_0 + \Delta u_0}{\alpha}\right) \sin(\alpha t). \end{aligned}$$

Thus, the separation between neighbouring trajectories at time  $t$  is,

$$\Delta x(t) = \Delta x_0 \cos(\alpha t) + \frac{\Delta u_0}{\alpha} \sin(\alpha t) = \Delta x_0 \left\{ \cos(\alpha t) + \frac{\theta_0}{\alpha} \sin(\alpha t) \right\}. \quad (16)$$

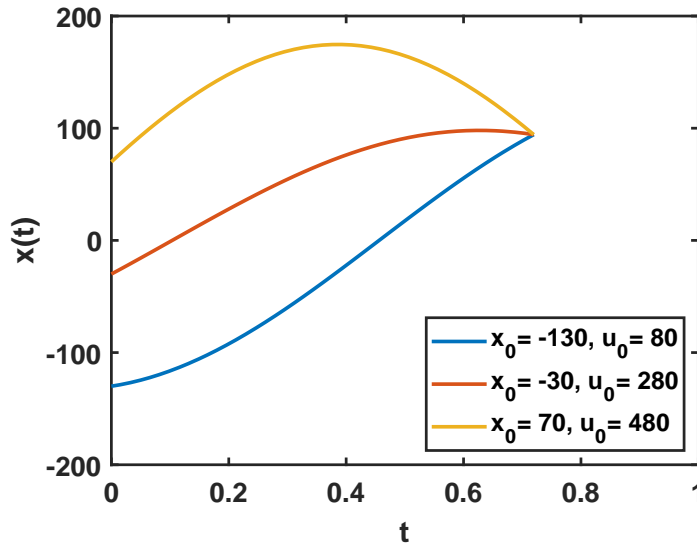


FIG. 3: Simple harmonic oscillator/simple pendula: Plots of trajectories for arbitrarily chosen values of the initial position ( $x_0$ ) and the initial velocity ( $u_0$ ). Here,  $\theta_0 = 2$  unit,  $\alpha = 3$  unit.

Let the trajectories meet at time  $t = t_f$  (see Figure 3). We have,

$$x_1(t_f) = x_2(t_f) \text{ or } \Delta x(t_f) = 0,$$

which gives, from Eqn. (13),

$$\theta_0 \tan(\alpha t_f) = -\alpha. \quad (17)$$

Thus, we obtain a relation between focusing time ( $t_f$ ) and initial expansion ( $\theta_0$ ). We can surely consider more than two pendula and adjust their initial positions and velocities in such a way that the initial value of expansion ( $\theta_0$ ) is the same for the family.

Further, one may obtain the above expression for  $t_f$  from the solution of the equation for  $\theta(t)$  given as,

$$\frac{d\theta}{dt} + \theta^2 = -\alpha^2. \quad (18)$$

It is straightforward to integrate this simple first order differential equation. The solution turns out to be [14],

$$\theta(t) = \alpha \left( \frac{\theta_0 - \alpha \tan(\alpha t)}{\alpha + \theta_0 \tan(\alpha t)} \right), \quad (19)$$

where the initial condition is  $\theta(t)|_{(t=0)} = \theta_0$ . Figure 4 shows the variation of  $\theta(t)$  with  $t$ .

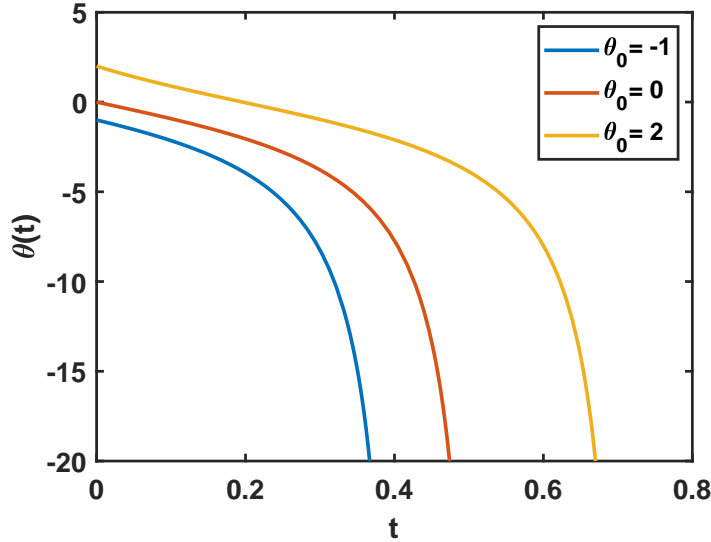


FIG. 4: Simple harmonic oscillator/simple pendula: Expansion  $\theta(t)$  for various  $\theta_0$ ,  $\alpha = 3$  units.

Since the condition for meeting of trajectories in finite time is  $\theta \rightarrow -\infty$  as  $t \rightarrow t_f$ , we find,

$$\theta_0 \tan(\alpha t_f) = -\alpha, \quad (20)$$

which is the same as (17).

Thus, the formula for the meeting time is given as,

$$t_f = \frac{1}{\alpha} \tan^{-1} \left( \frac{-\alpha}{\theta_0} \right). \quad (21)$$

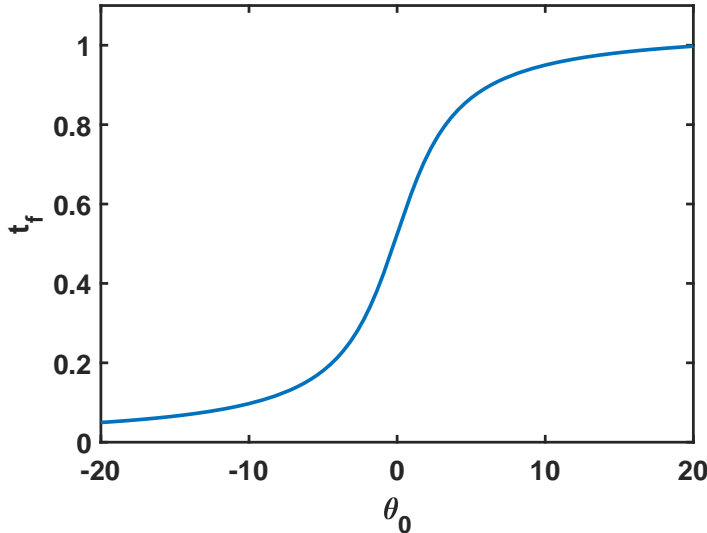


FIG. 5: Simple harmonic oscillator/simple pendula: Meeting/focusing time ( $t_f$ ) with initial expansion ( $\theta_0$ ),  $\alpha = 3$  units.

As the tangent function can have any value between  $-\infty$  to  $\infty$ , trajectories will meet for all values of the initial expansion ( $\theta_0$ ) and  $\alpha$ . Figure 5 shows the variation of  $t_f$  with  $\theta_0$ .

### III. EXPERIMENTS

We now set up an experiment involving simple pendula with the aim of learning whether our theoretical model and its quantitative predictions can explain the experimental observations. In particular, the meeting/ focusing time is one quantity which we obtain in our model and also measure in the experiment.

#### A. Practical considerations

A practical realization of the theoretical model, discussed above, demands a modification in the given expression for  $t_f$  due to finite size of the bobs of the pendula and a careful look at the issue of air-damping, which we elaborate below.

1. *Finite size-correction for meeting/focusing time*

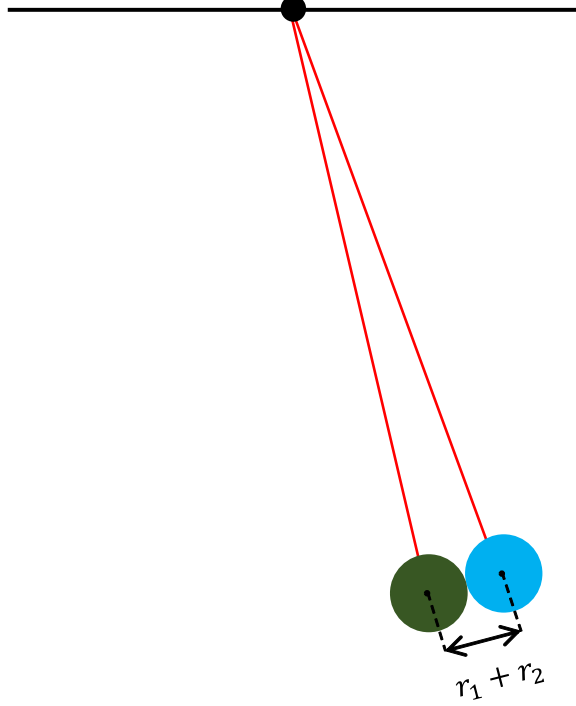


FIG. 6: Finite-size correction

In Section II, the theory was developed assuming point masses representing the bobs of the simple pendula. For practical purposes, the bob of a simple pendulum is of finite size. In the derivation of Equation 21, the focusing/meeting of two trajectories occur when the separation between point particles becomes identically zero. In practice, when two bobs meet, they do so at their boundaries and not at their centers of mass (see Figure 6). Thus, Equation 21 needs to be modified for this finite-size effect.

Let us assume that we have two bobs with initial positions  $x_{01}$ ,  $x_{02}$  and initial velocities  $u_{01}$ ,  $u_{02}$  respectively. Following Equation 14, the positions of these bobs after some time  $t$  can be written as,

$$\begin{aligned} x_1(t) &= x_{01} \cos(\alpha t) + \left( \frac{u_{01}}{\alpha} \right) \sin(\alpha t), \\ x_2(t) &= x_{02} \cos(\alpha t) + \left( \frac{u_{02}}{\alpha} \right) \sin(\alpha t), \end{aligned}$$

where,  $\alpha = \sqrt{\frac{g}{l}}$ , and  $l$  is length of the pendula. When they strike/meet, the separation between them is equal to the sum of their radii, i.e.

$$|x_2(t'_f) - x_1(t'_f)| = r_1 + r_2, \quad (22)$$

where,  $r_1$  and  $r_2$  are the radii of the bobs. Using the above-stated expressions for  $x_1(t)$ ,  $x_2(t)$  in Equation 22, we obtain

$$|(x_{02} - x_{01}) \cos(\alpha t'_f) + \left(\frac{u_{02} - u_{01}}{\alpha}\right) \sin(\alpha t'_f)| = r_1 + r_2 \quad (23)$$

Since the initial expansion  $\theta_0 = \frac{u_{02} - u_{01}}{x_{02} - x_{01}}$ , we rewrite Equation 23 as

$$|(x_{02} - x_{01})| \left| \cos(\alpha t'_f) + \frac{\theta_0}{\alpha} \sin(\alpha t'_f) \right| = r_1 + r_2 \quad (24)$$

Therefore, we have

$$\left| \cos(\alpha t'_f) + \frac{\theta_0}{\alpha} \sin(\alpha t'_f) \right| = A = \frac{r_1 + r_2}{|x_{02} - x_{01}|} \quad (25)$$

where  $0 < A < 1$ , which follows from the requirement  $0 < r_1 + r_2 < |x_{02} - x_{01}|$  (i.e. initial separation always greater than sum of radii).

Squaring both sides of Equation 25 we obtain,

$$\left(\frac{\theta_0^2}{\alpha^2} + 1\right) \sin^2(\alpha t'_f) - \frac{2A\theta_0}{\alpha} \sin(\alpha t'_f) + A^2 - 1 = 0 \quad (26)$$

which is a quadratic in  $\sin(\alpha t'_f)$  and can be easily solved to get  $t'_f$  as,

$$t'_f = \frac{1}{\alpha} \sin^{-1} \left[ \alpha \cdot \left\{ \frac{A \cdot \theta_0 + \sqrt{(\theta_0^2 + \alpha^2 - A^2 \cdot \alpha^2)}}{\theta_0^2 + \alpha^2} \right\} \right] \quad (27)$$

The other solution of the quadratic, given as,

$$t'_f = \frac{1}{\alpha} \sin^{-1} \left[ \alpha \cdot \left\{ \frac{A \cdot \theta_0 - \sqrt{(\theta_0^2 + \alpha^2 - A^2 \cdot \alpha^2)}}{\theta_0^2 + \alpha^2} \right\} \right] \quad (28)$$

is discarded since it gives a negative  $t'_f$  ( $0 < A < 1$ ).

Thus, in practice, the meeting/focusing time depends not only on the value of the initial expansion ( $\theta_0$ ) and  $\alpha$  (as in Equation 21), but also on the value of  $A$ . In the limiting case when  $r_1 = r_2 = 0$  (or  $A = 0$ ), Equation 27 reduces to Equation 21 (focusing time when the bobs are point particles).

## 2. Air-damping

In reality, the oscillation of a pendulum is damped by air. To calculate the damping constant ( $\beta$ ), we studied the successive oscillation of one of the two identical pendula, used in

our main experiment. From the logarithmic decrement of the successive amplitudes of the damped simple harmonic oscillator, the value of the damping constant ( $\beta$ ) is estimated to be  $(0.00309 \pm 0.00005) \text{ sec.}^{-1}$ . This value is very small as compared to the angular frequency ( $\alpha$ ), which is  $(3.260 \pm 0.002) \text{ rad. sec.}^{-1}$  (see next section for its measurement). Thus, in our experimental results, we ignored the contribution of air-damping while obtaining the trajectories of the pendula.

## B. Experimental Setup

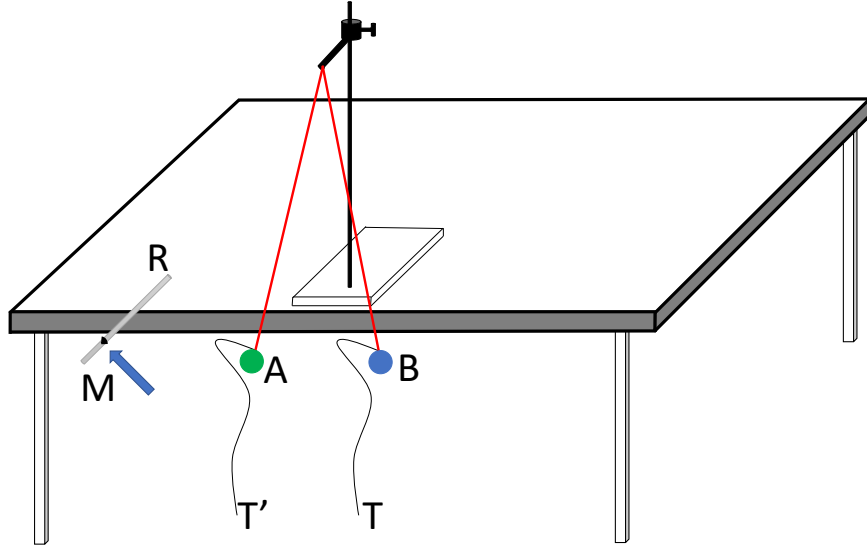


FIG. 7: Schematic diagram of the experimental setup. A and B: Pendula, R: Rod, M: marking on the rod and, T and T': threads attached to the bobs of the pendula.

Figure 7 shows the schematic diagram of our simple setup. In our experiment, we took two pendula (A and B in Figure 7). The bobs of the pendula were of nearly equal size ( $24.94 \pm 0.02 \text{ mm}$  and  $24.82 \pm 0.02 \text{ mm}$ ) and weight ( $70.821 \pm 0.001 \text{ gm}$  and  $71.020 \pm 0.001 \text{ gm}$ ). The length of each pendulum was nearly equal ( $92.2 \pm 0.1 \text{ cm}$ ) [15]. The angular frequency  $\alpha$  can be found from the length of each pendula and is, as stated above  $(3.260 \pm 0.002) \text{ rad. sec.}^{-1}$ . We have also checked the angular frequency from a direct measurement of the time period of oscillation, and the difference between the value found and that obtained from the length is insignificant. To keep the motion of two bobs in the same plane, we fixed a marked steel rod (R in Figure 7) on the table. The marking (M) on the rod and the equilibrium

position of the bobs were at the same distance from the side of the table. We fixed thin threads (T and T') on both bobs.

### C. Measurements

To set the motion, threads T and T' were pulled at mark M and then released one after the other. To achieve different initial velocities for two bobs, one of them was first released from the mark M on the rod. When it attained a certain velocity in its trajectory, the bob of the other pendulum was released from the same mark M. The time difference between the release of the first and second bobs was varied to generate trajectories of the pendula with different sets of values for  $x_{01}$ ,  $x_{02}$ ,  $u_{01}$ , and  $u_{02}$ . The trajectories of both bobs were recorded simultaneously using a wireless camera that can record 60 frames per second. It is to be noted that since we will be dealing with instantaneous positions and velocities of the two pendula, the origin of their trajectories is not relevant.

#### 1. *Measurement of position and time*

To obtain the positions of the bobs, we processed the video using OpenCV Python code [16, 17]. Two bobs were painted with different colors, green and blue. After removing the background using a bandpass filter, the program differentiated two bobs following the HSV (hue, saturation and value) code. The code chose the planar projection of the spherical balls and defined the center of the corresponding circles which determined the position of their centers on their trajectories. From the code, we obtained the position of the center of mass of the two bobs with respect to the equilibrium positions. To convert it into a real physical unit of length, we measured the diameter of one of the bobs using slide-caliper and by the code. The estimated conversion factor, obtained from the ratio of these values, was used throughout the experiment to study the trajectories of the bobs in a real physical unit. This conversion factor also defines the length corresponding to one pixel and is used as the error in position measurements.

As mentioned above, the video was recorded with 60 frames per second. By counting the number of frames between two desired positions of the bobs, the total time lapse could be estimated. The error in our measurement of time is 1/60 second.

## 2. Measurements of velocity

We assume the motion only along a line (say x-axis), and get the value of x-position at subsequent times using the code. Next, we use the central difference method to determine its velocity (which is the derivative of position with respect to time). Note that, if we have the value of a function  $f(x)$  at  $x_i$ ,  $x_i - h$  and  $x_i + h$ , then its first derivative at  $x = x_i$  to first order of  $h$ , is given by,

$$f'(x_i) = \frac{f(x_i - h) + f(x_i + h)}{2h}. \quad (29)$$

In our case, with the known value of the position at time  $t_i$ ,  $t_i - h$  and  $t_i + h$ , the velocity at  $t = t_i$  to first order in  $h$ , is given by,

$$v(t_i) = \dot{x}(t_i) = \frac{x(t_i - h) + x(t_i + h)}{2h}, \quad (30)$$

where, a dot denotes a first derivative w.r.t. time. Note that we recorded the video with 60 frames per second. The positions can be obtained for each  $h = \frac{1}{60}$  sec.

## IV. THEORETICAL MODEL VERSUS EXPERIMENTAL FINDINGS

We now compare the  $t'_f$  values found in our theoretical model and the experimentally observed meeting/focusing time for different values of initial expansion ( $\theta_0$ ). In Figure 8 the experimental data points are shown by square symbols. The solid blue line plots the expected variation of the focusing time without the size correction following Equation 21. The red open symbols represent values obtained from Equation 27, after including the size correction to the meeting/focusing time. It is to be noted that the theoretical model based plot with the size correction is not a smooth curve as the parameter  $A$  in Equation 27 does not have a constant value. It depends on the  $x_{02} - x_{01}$  for a given value of  $\theta_0$  (Equation 25). A fairly good agreement between the theoretical model based values and the experimental data validates the predicted expression for  $t'_f$  (Equation 27).

We also obtain the expansion of trajectories,  $\theta(t)$ , as a function of time, for both positive and negative initial values of  $\theta$ , i.e.,  $\theta_0$ . The symbols in Figure 9 (a) and (b) plot the experimental data points for a negative and a positive value of  $\theta_0$ , respectively. The theoretical model based plots following Equation 19 are shown by the solid lines in these figures. The trajectories of the two bobs for the above values of  $\theta_0$  are shown in Figure 9 (c) and (d).

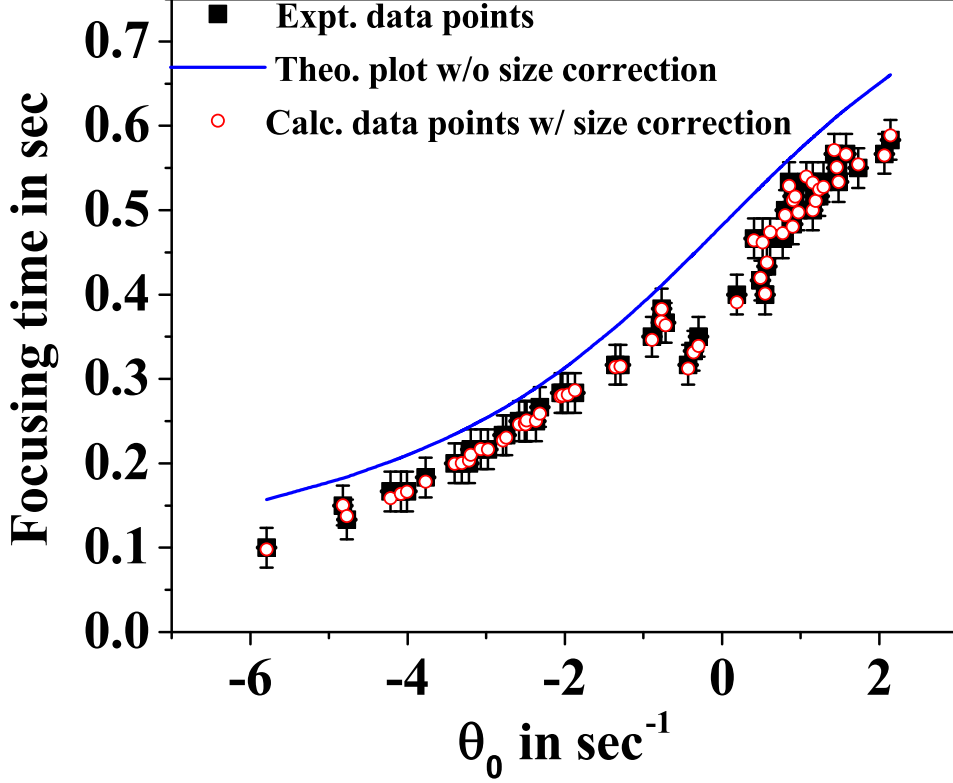


FIG. 8: Variation of meeting/focusing time with initial expansion.

Here too, the experimental data are shown by symbols in the graphs, and the theoretical model based trajectories following Equation 14 are shown by the solid lines. It is important to note that the trajectories in Figures 9 (c) and 9 (d) do not exactly meet. The reason for this is the finite-size correction discussed in detail earlier.

## V. ANALOGY

As mentioned in Section I, the meeting/focusing time of trajectories derived above in the mechanics example and thereafter realised in an experiment, is analogous to the notion of focusing of geodesics in Riemannian geometry/gravitational physics. Let us now explain how the analogy works. [14].

To obtain the Raychaudhuri equations in Riemannian geometry, we use the gradient of the normalised, timelike four-velocity field  $u^i$  ( $u_i u^i = -1$ ), given by  $\nabla_j u_i$ . Here  $\nabla_j$  is the covariant derivative,  $u_i = g_{ij} u^j$  and  $g_{ij}$  is the component of the metric tensor in the line

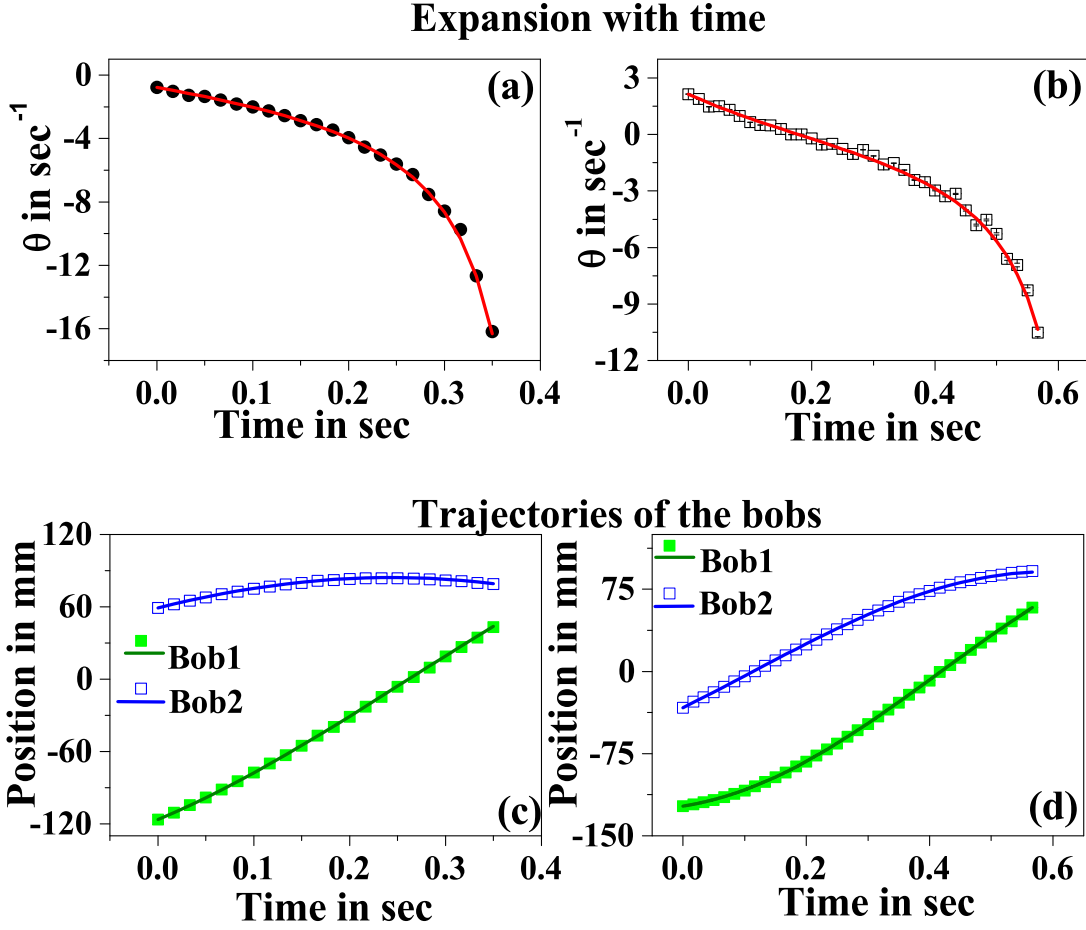


FIG. 9: Variation of expansion with time for (a) a negative value of  $\theta_0$  (filled black symbol), (b) a positive value of  $\theta_0$  (open black symbol). The calculated values of the same using Equation 19 are shown by solid red lines. In (c) and (d), the trajectories of two bobs corresponding to (a) and (b), respectively, are shown by green and blue symbols. The same as could be estimated from Equation 14 are shown by the solid lines. The error bars [15] for the experimental data are within the size of the symbols.

element  $ds^2 = g_{ij}dx^i dx^j$ .  $\nabla_j u_i$  is a tensor of rank two and can therefore be decomposed into its trace, symmetric traceless, and antisymmetric parts which represent, respectively, the isotropic expansion, shear and rotation of the congruence (for more details see [5–8]). The trace of  $\nabla_j u_i$ , given as  $\nabla_j u^j$  is defined as the expansion ( $\theta$ ), which, for one dimensional mechanics is just  $\frac{\partial u}{\partial x}$  (Equation 2) [8], a quantity we have introduced and named as  $\theta$ . The Raychaudhuri equation for the expansion of a timelike geodesic congruence follows from

| Mechanical systems  | General Relativity  |
|---|---|
| Parameter: time (t)   | Parameter: $\lambda$ (affine, non-affine)   |
| Trajectories  | Geodesics   |
| Family of trajectories  | Congruence of geodesics<br>(timelike and null)  |
| Meeting of trajectories   | Geodesic focusing   |
| Time of meeting   | Value of parameter $\lambda$ at focal point   |
| $\theta(t) = \frac{\partial u}{\partial x}$   | Expansion (Trace $(\nabla_j u_i)$ )   |
| Equation for $\theta(t)$ (one dimension)<br>$\frac{d\theta}{dt} + \theta^2 = -\frac{\partial^2 V}{\partial x^2} = f(t)$ | Equation for $\theta(\lambda)$ (three dimensions, timelike)<br>$\frac{d\theta}{d\lambda} + \frac{1}{3}\theta^2 = -\sigma^2 + \omega^2 - R_{ij}u^i u^j = g(\lambda)$ |

TABLE I: The analogy summarised.

an evaluation of  $u^k \nabla_k (\nabla_j u_i)$ , which is the generalisation of the quantity  $u \frac{\partial}{\partial x} \left( \frac{\partial u}{\partial x} \right)$ , for higher dimensions and curved spacetimes [3, 5–8]. The equation for  $\theta$  is given as:

$$\frac{d\theta}{d\lambda} + \frac{1}{3}\theta^2 = -R_{ij}u^i u^j - \sigma_{ij}\sigma^{ij} + \omega_{ij}\omega^{ij} = g(\lambda) \quad (31)$$

where,  $\lambda$  is a parameter,  $\omega_{ij}$  is the antisymmetric rotation tensor,  $\sigma_{ij}$  is the symmetric traceless shear tensor and  $R_{ij}$  is the Ricci tensor (for a definition of the Ricci tensor and a derivation of the above equation see [5, 6]). The focusing theorem follows by assuming  $\omega_{ij} = 0$  and  $R_{ij}u^i u^j \geq 0$ , reducing the equation to an inequality  $\frac{d\theta}{d\lambda} + \frac{1}{3}\theta^2 \leq 0$ . Integrating the inequality leads to the conclusion that  $\theta \rightarrow -\infty$  within a finite  $\lambda$  [5, 6].

Recall that the equation for the expansion ( $\theta$ ) in one dimensional mechanical systems was (as shown in Equation 5),

$$\frac{d\theta}{dt} + \theta^2 = -\frac{\partial^2 V}{\partial x^2} = k(t) \quad (32)$$

Looking at Equation 31 and Equation 32 one can easily notice similarities. In Equation 31,  $\lambda$  is a parameter and in Equation 32,  $t$  is an external parameter. In the second term of Equation 31 there is a  $\frac{1}{3}$  factor arising due to three space dimensions. In Equation 32 this factor is just one, as we work in only one space dimension. Finally, the R.H.S. term is a function of the parameter ( $t$  or  $\lambda$ ) in both equations. It may be noted that in mathematics, such equations are known as Riccati equations [18]. Thus, the parallels between (a) the various quantities, (b) the equation for mechanical systems and the one in Riemannian

geometry and (c) the resultant notion of meeting of trajectories/focusing are quite easily seen. We do seem to have an *analog Raychaudhuri equation* in mechanics. The analogy is summarised in Table I.

How is such an analogy useful? First and foremost, it is a tool to introduce the basic elements of the Raychaudhuri equation and the focusing theorem to those who may not be familiar with it. Next, it is possible that the analog equation (as well as its higher dimensional generalisations in mechanics), can be investigated as an equation in its own right with the motivation of learning about collisions as well as avoidance in a family of trajectories. Finally, solutions of the analog equation in mechanics can lead us towards developing criteria on initial conditions for invoking avoidance in a family of trajectories. Such an approach (though not carried out yet) may be relevant in the context of conjunction assessment and risk analysis programmes associated with artificial satellites, as explained in [21].

## VI. CONCLUDING REMARKS

Let us now conclude with some possible avenues of future work.

It is certainly possible to go beyond the simple experiment discussed here. A straightforward extension is to study systems where drag forces are present. For example, the simple experiment related to Stokes' law [2] may be modified to perform a study similar to what has been done here. The theoretical model and its details appear in [14]. Further, one may go beyond one dimension. Here too the theory has been developed [14] and applied to projectile motion [1, 2], which, may be studied experimentally. The basic idea would be to shoot several projectiles from different positions at different velocities and obtain, using videography, the positions of each projectile at subsequent times. One can study the evolution of expansion, shear and rotation in this example and find out how the meeting/focusing time varies with initial conditions.

Moving away from mechanics, a formal study of families of trajectories also has useful applications in elasticity and fluids, as briefly indicated in [6]. More elaborate discussion along these lines (especially the occurrence of caustics and vortices in media) may be possible following the detailed framework provided in [19, 20].

In conclusion, our present work is only a beginning. The future aim is to broaden the

scope of mechanics through studies on families of trajectories as opposed to individual ones. The immediate outcome of these studies is its direct link with a topic usually discussed in the context of Riemannian geometry and General Relativity. It remains to be seen whether such analyses have useful applications in mechanical systems. At the very least, this novel approach surely provides a simple and worthwhile analog which may be used while introducing the basics of the Raychaudhuri equation and its consequences. Moreover, through the experiments reported here, we have probably, for the first time, found a way to *realise in a laboratory experiment* a rather involved concept like *focusing of trajectories*, through this analogy.

### Acknowledgements

We would like to thank Anang Kumar Singh and Kushal Lodha for their help in the experimental part. RPB thanks Department of Physics, IIT Kharagpur where he was a student in the Master of Science programme, when this work was carried out.

- 
- [1] K. R. Symon, *Mechanics*, Addison-Wesley Publishing Company (1971).
  - [2] D. Kleppner and R. Kolenkow, *An Introduction to Mechanics*, Cambridge University Press (2014).
  - [3] A. Raychaudhuri, *Relativistic cosmology I*, Phys. Rev. **98**, 1123 (1955).
  - [4] A clear exposition of Raychaudhuri's original method of deriving the Raychaudhuri equation (for timelike congruences) appears in E. Witten, *Light rays, singularities and all that*, arXiv:1901.03928.
  - [5] R. M. Wald, *General Relativity*, University of Chicago Press, United States (1984).
  - [6] E. Poisson, *A Relativist's Toolkit: The mathematics of black hole mechanics*, Cambridge University Press (2004).
  - [7] S. Kar and S. SenGupta, *The Raychaudhuri equations: a brief review*, Pramana **69**, 49 (2007).
  - [8] S. Kar, *An introduction to the Raychaudhuri equations*, Resonance, journal of science education **13**, 319 (2008).
  - [9] R. Penrose, *Gravitational collapse and space-time singularities*,

- Phys. Rev. Letts. **14**, 57 (1965).
- [10] S. W. Hawking and R. Penrose, *The nature of space and time*, Princeton University Press (1996).
  - [11] S. W. Hawking and G. F. R. Ellis, *The large scale structure of space-time*, Cambridge University Press, Cambridge, UK (1973).
  - [12] The equations for null geodesic congruences were derived in R. Sachs, *Gravitational waves in general relativity VI. The outgoing radiation condition*, Proc. R. Soc. Lond. **A 264**, 309 (1961).
  - [13] V. Perlick, *Gravitational lensing from a spacetime perspective*, Living Rev. Relativ. **7**, 9 (2004).
  - [14] R. Shaikh, S. Kar and A. DasGupta, *Kinematics of trajectories in classical mechanics*, EPJP **129**, 90 (2014); arXiv:1312.0071v2.
  - [15] J. R. Taylor, *An introduction to error analysis*, University Science Books, Chapter 1-3 (1997).
  - [16] A. Rosebrock, *Ball Tracking with OpenCV*, pyimagesearch, September 14, 2015.
  - [17] A. Rosebrock, *Measuring size of objects in an image with OpenCV*, pyimagesearch, March 28, 2016.
  - [18] E. L. Ince, *Ordinary differential equations*, Dover Publications (1978).
  - [19] V. Červený, and F. Hron, *The ray series method and dynamic ray tracing system for three-dimensional inhomogeneous media*, Bull. Seismol. Soc. Am. **70**, 47 (1980).
  - [20] V. Červený, *Seismic ray theory*, Cambridge University Press (2001).
  - [21] See for example *Satellite Safety*, CARA, NASA, USA.